

Supplemental information

Single-cell-resolved interspecies comparison

shows a shared inflammatory axis and a dominant

neutrophil-endothelial program in severe COVID-19

Stefan Peidli, Geraldine Nouailles, Emanuel Wyler, Julia M. Adler, Sandra Kunder, Anne Voß, Julia Kazmierski, Fabian Pott, Peter Pennitz, Dylan Postmus, Luiz Gustavo Teixeira Alves, Christine Goffinet, Achim D. Gruber, Nils Blüthgen, Martin Witzernrath, Jakob Trimpert, Markus Landthaler, and Samantha D. Praktijn

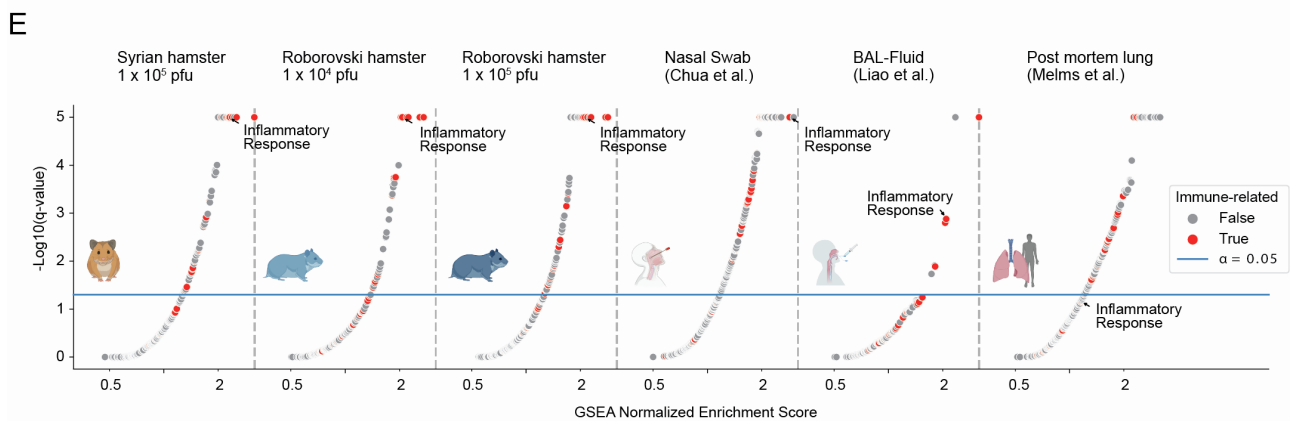
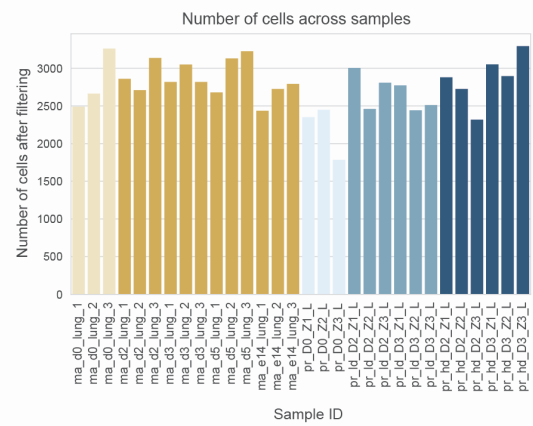
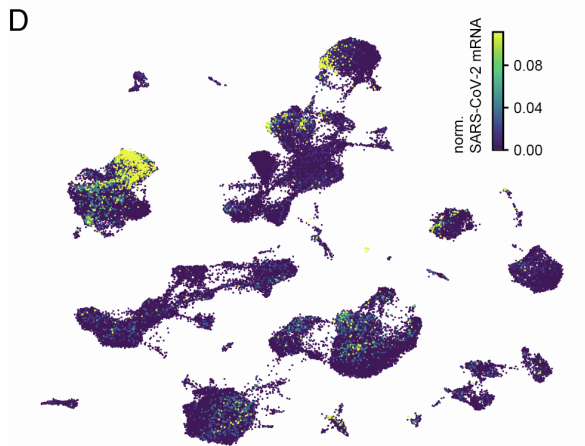
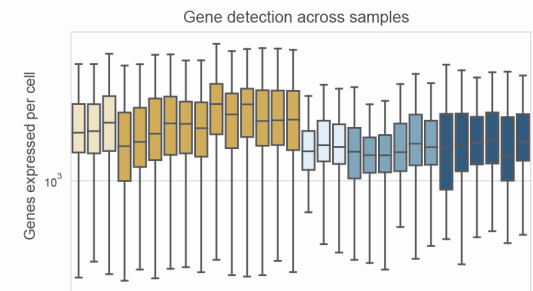
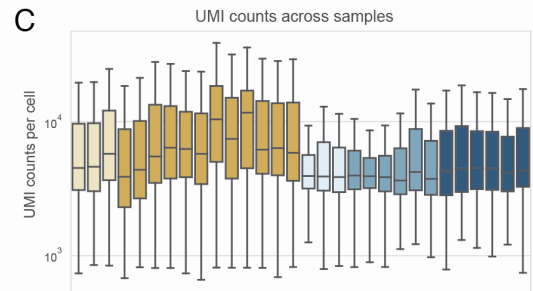
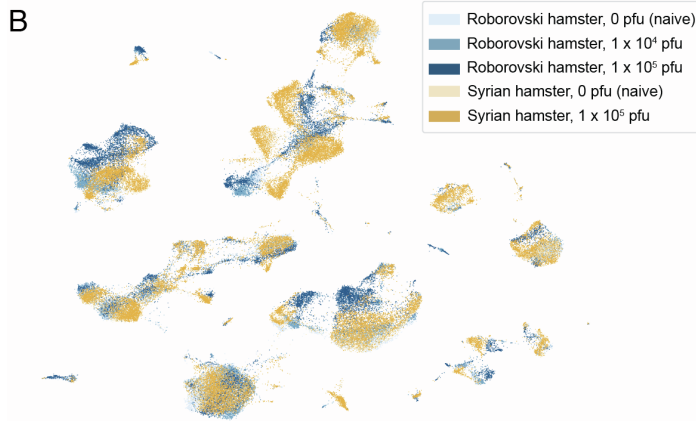
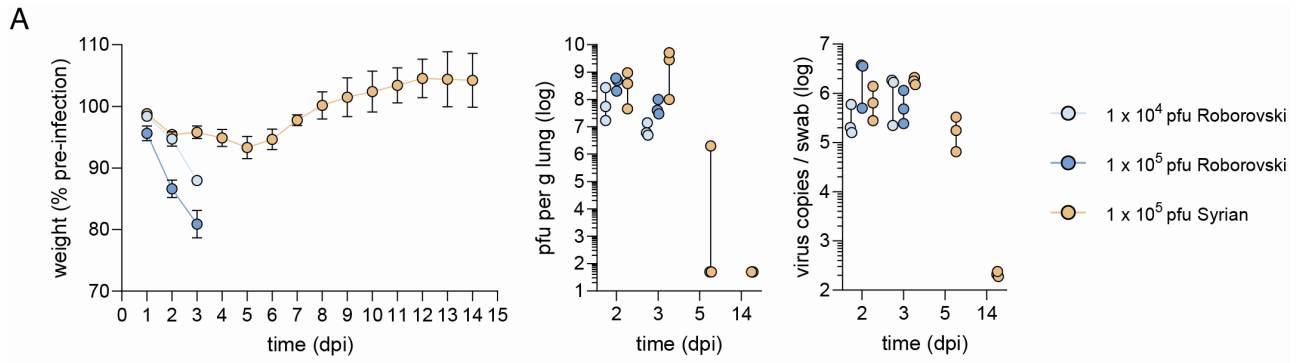


Figure S1. Clinical data, scRNA-seq data statistics, upregulated gene sets across datasets. (A) Weight w.r.t. pre-infected (left), log-scale virus pfu per gram lung tissue (middle), and log-scale virus copies per swab (right) colored by study branch (hamster type and virus dose) along dpi (clinical data previously published^{18,19}). Data are represented as mean \pm SEM. (B) UMAP embedding of integrated datasets colored by hamster species and virus dose. (C) UMI counts (top), number of genes with at least one UMI count (middle) per cell and number of cells after filtering (bottom) per sample colored by hamster species and virus dose. (D) UMAP embedding as in B showing normalized SARS-CoV-2 mRNA sequence counts per cell. (E) GSEA across datasets based on DEGs from DESeq2 testing infected (2 and 3 dpi) vs. control showing upregulated gene sets with immune-related terms indicated in red. Normalized Enrichment Score (NES) as x-axis and $-\log_{10}(\text{q-value})$ as y-axis. Blue line corresponds to a q-value of 0.05.

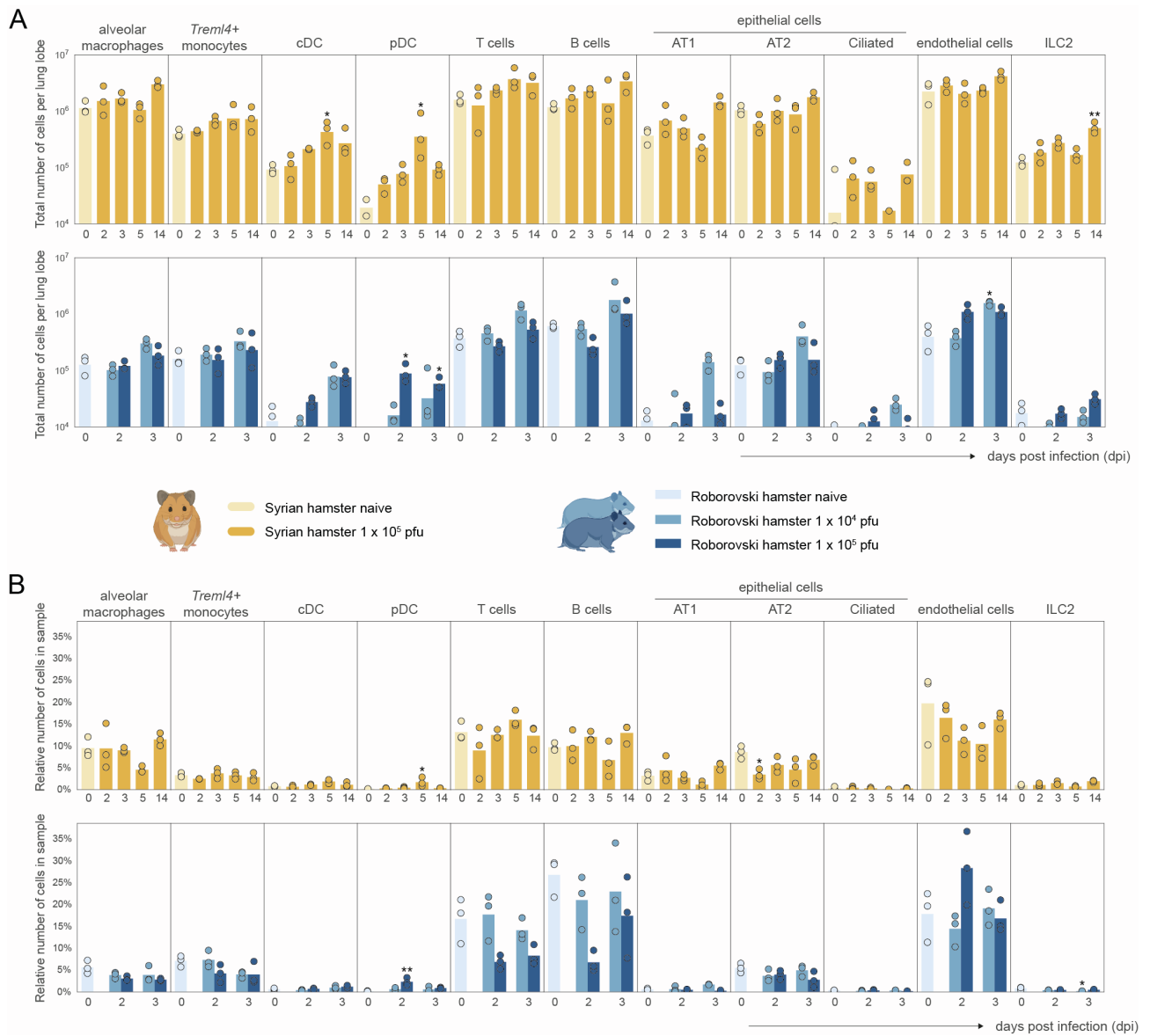


Figure S2. Cell numbers across all other annotated cell types. (A) as in Figure 2B. (B) as in Figure 2C.

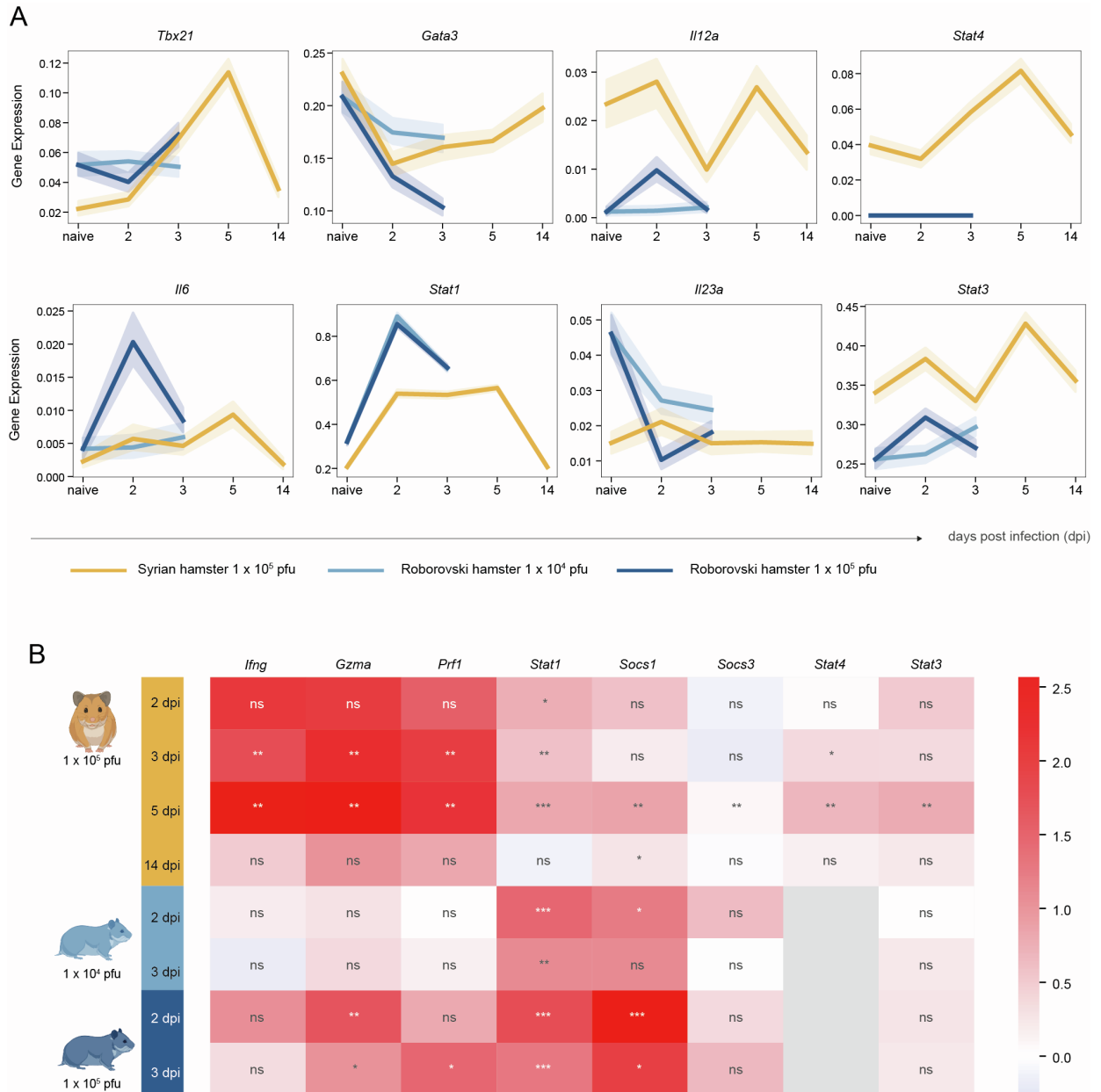


Figure S3. Selected gene expression along time after infection. (A) Expression time courses along time after infection per species and virus dose combination for selected immunity marker genes. **(B)** Sample-wise log₂ fold-changes of normalized expression with respect to corresponding uninfected samples for selected genes after pseudobulking T cell, NK cell and ILC2 clusters. P-values of t-test for difference in significance across samples (n=3) marked with * < 0.05 , ** < 0.01 or ns: not significant.

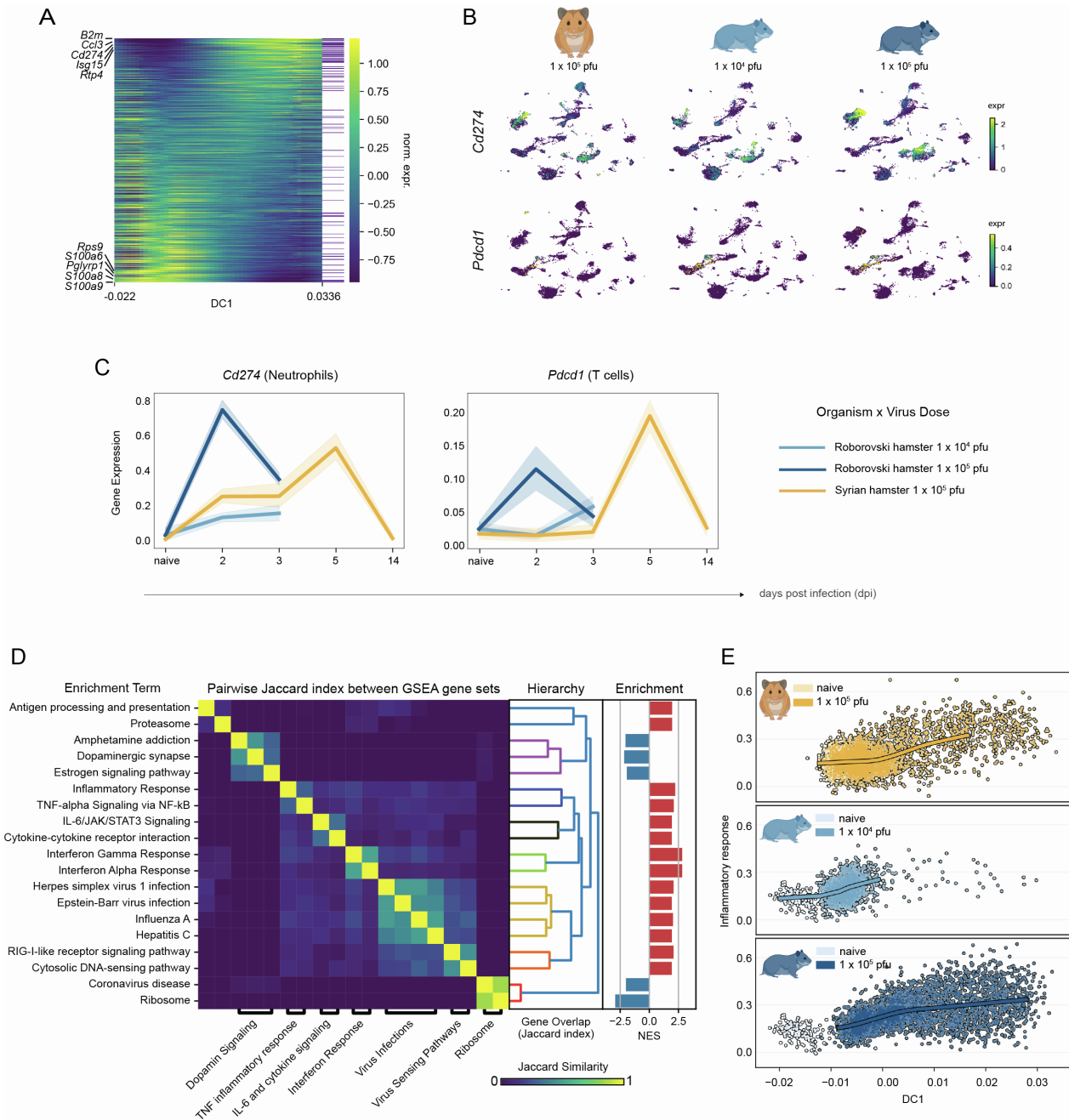


Figure S4. Supporting analyses for neutrophil response to infection. (A) Expression of top 100 (anti-) correlating genes along DC1 with genes belonging to the inflammatory response gene set indicated by a purple line in the right column of the heatmap. **(B)** UMAP embeddings of all cells colored by expression of *Cd274* (top) and *Pdccl1* (bottom), split by hamster type and virus dose. **(C)** Gene expression trends of *Cd274* in neutrophils and *Pdccl1* in T cells along time before and after infection per hamster type and virus dose. Areas around curves are 95% confidence intervals by bootstrapping. **(D)** Pairwise Jaccard index between leading edge gene sets reported by GSEA on DC1 correlating genes. Jaccard index measures the overlap between sets; a value of 1 corresponds to perfect overlap. Resulting hierarchy and associated normalized enrichment scores from GSEA adjacent to the right. Bottom: annotation of heatmap aggregates similar gene sets with high overlap to reduce redundancy. **(E)** Neutrophil DC1 against inflammatory response score split by species and virus dose, colored by infection status. LOESS regression lines shown on top.

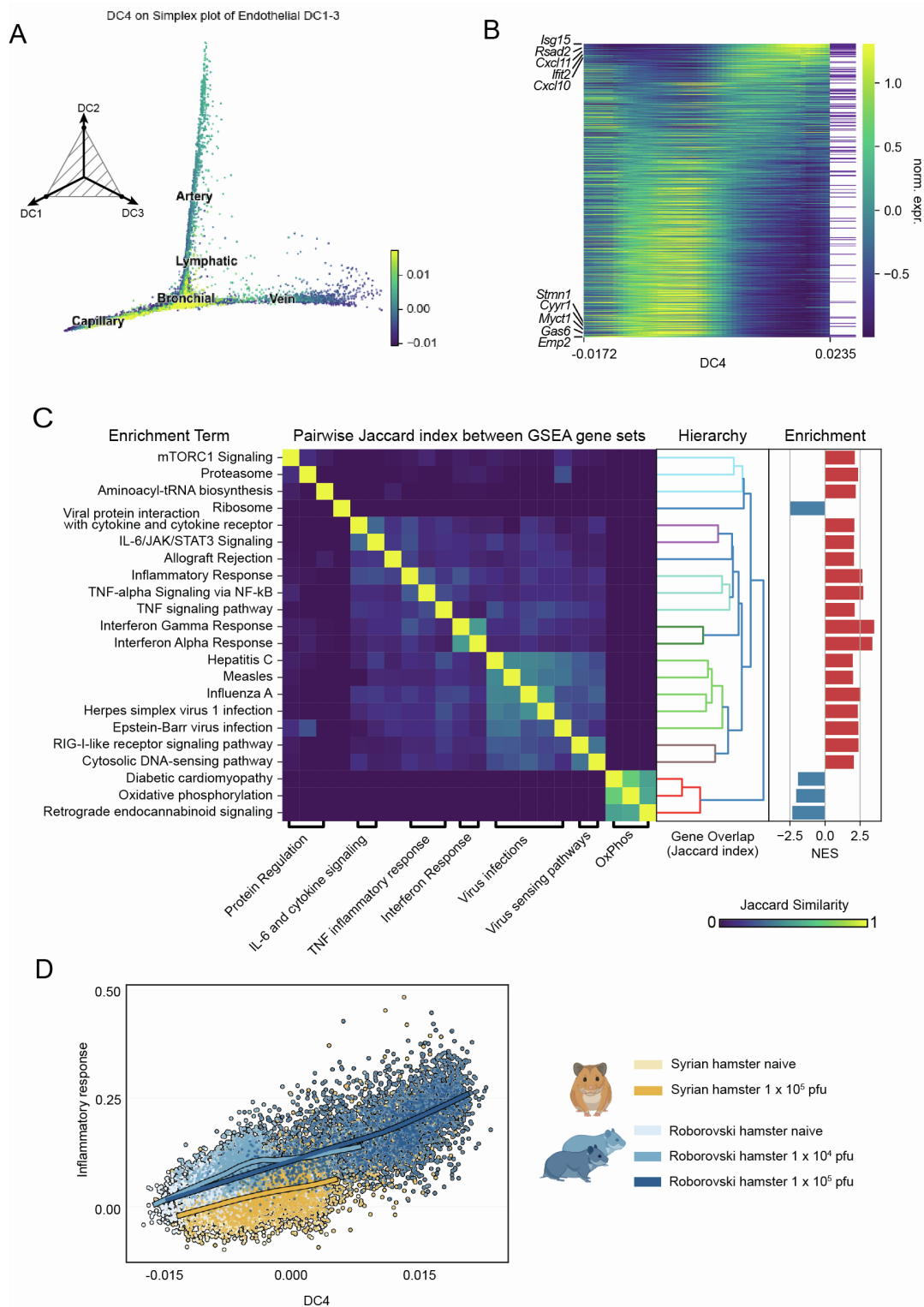


Figure S5. Supporting analyses for endothelial cell response to infection. (A) Simplex plot from Figure 5A colored by DC4 value of endothelial cells shows response primarily by capillary and bronchial subtypes. (B) Expression of top 100 (anti-) correlating genes along DC1 with genes belonging to the inflammatory response gene set indicated by a purple line in the right column of the heatmap. (C) Pairwise Jaccard index between leading edge gene sets reported by GSEA on DC4 correlating genes. Jaccard index measures the overlap between sets; a value of 1 corresponds to perfect overlap. Resulting hierarchy and associated normalized enrichment scores from GSEA adjacent to the right. Bottom: annotation of heatmap aggregates similar gene sets with high overlap to reduce redundancy. (D) Endothelial DC4 against inflammatory response score colored by species and virus dose. LOESS regression lines shown on top.

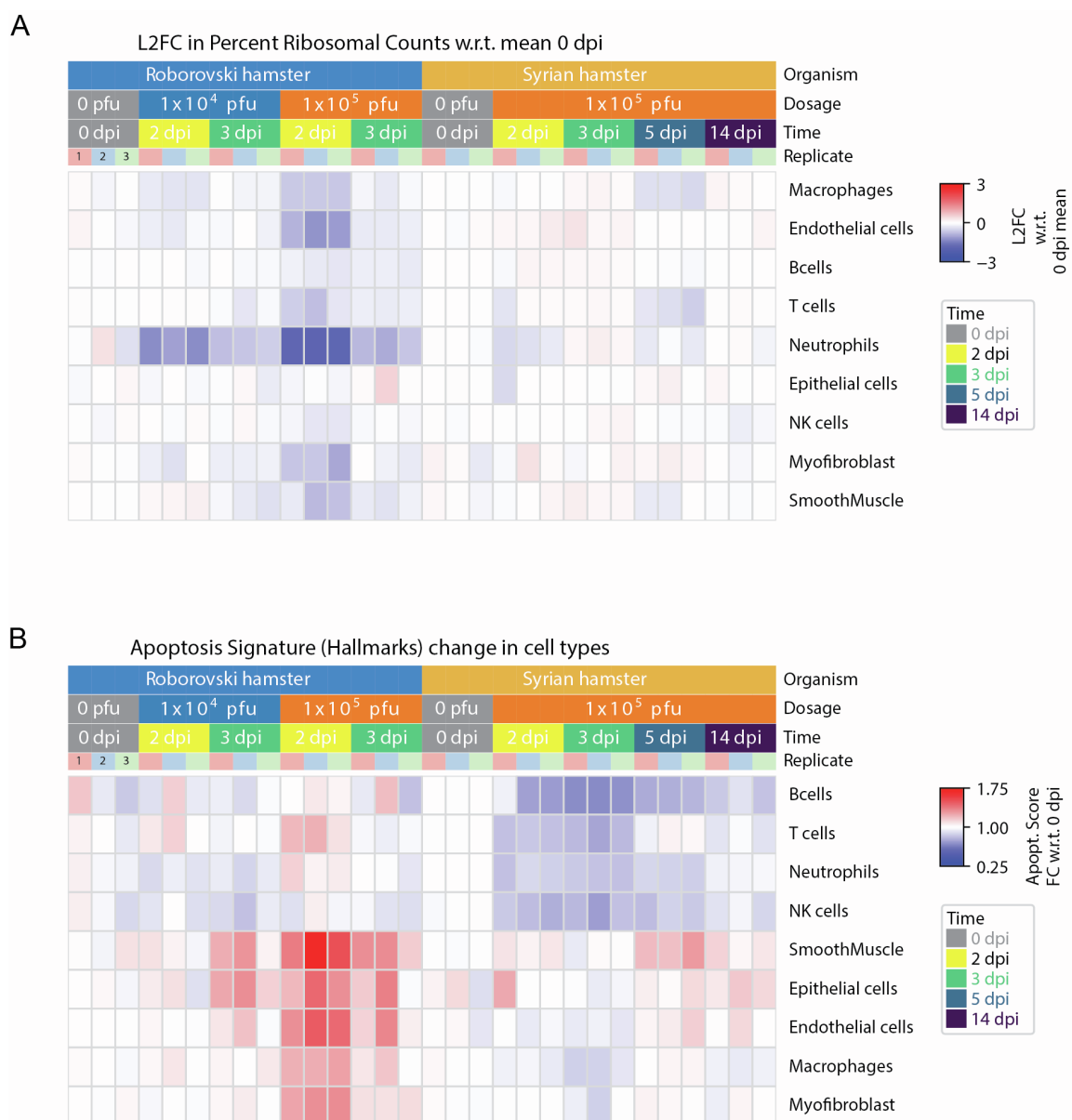


Figure S6. Selected gene signatures per cell type. (A) Sample-wise log2 fold-change in the relative abundance of UMI counts from ribosomal genes with respect to 0 dpi mean per main cell type. Cell types with less than 1000 cells in total across all samples and hamster types were excluded. (B) Fold-change in apoptosis signature score (Hallmarks from MsigDB⁶³) with respect to 0 dpi sample average per main cell type and grouped by sample type. Complete data for (A) and (B) are available in Table S6 (see source files as listed in the key resources table).

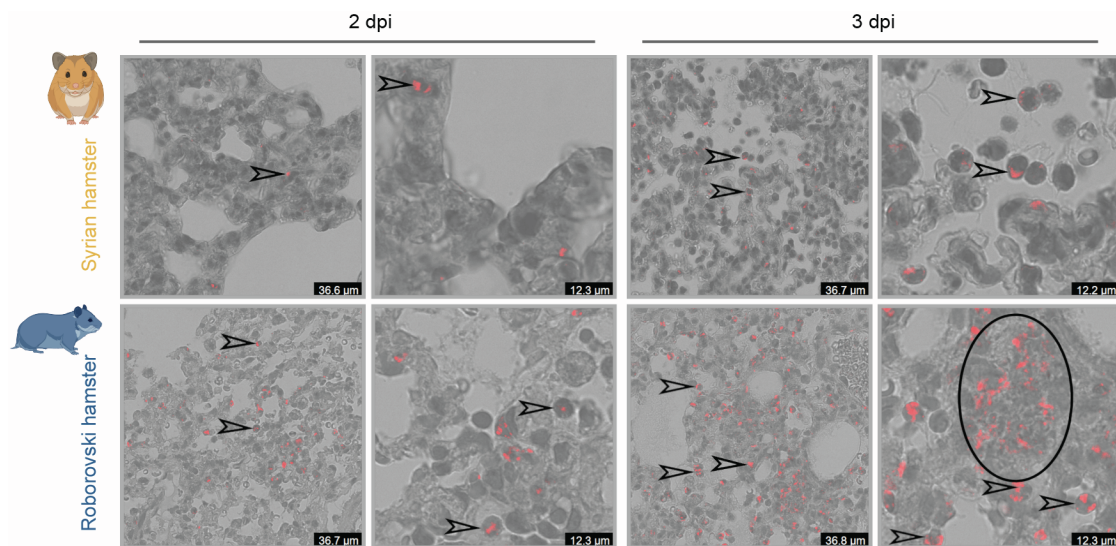


Figure S7. Histopathological examination of neutrophils by NACE stain. At 2 dpi, reactive neutrophils (open arrowheads, red signals) with round to oval cell shape and polymorphic nuclei were less numerous in the alveolar air space in Syrian hamsters (top) than in Roborovski hamsters (bottom). At 3 dpi, multiple areas with frayed staining signals (oval) suggesting the presence of undefined cell borders, cell debris accumulation, erythrocytes, and pycnotic nuclei in the Roborovski hamster. Naphthol AS-D chloroacetate esterase (NACE) pictured in red with original magnification at 630-fold and three-fold digitally zoomed-in photomicrographs.